

Carbon-Enhanced Metal-Poor Stars. Osmium and Iridium Abundances in the Neutron-Capture-Enhanced Subgiants CS 31062–050 and LP 625–44¹

Wako Aoki², Sara Bisterzo^{3,4}, Roberto Gallino^{3,5}, Timothy C. Beers⁶, John E. Norris⁷, Sean G. Ryan^{8,9}, Stelios Tsangarides⁸

ABSTRACT

We have investigated the abundances of heavy neutron-capture elements, including osmium (Os) and iridium (Ir), in the two Carbon-Enhanced Metal-Poor (CEMP) subgiants CS 31062–050 and LP 625–44. CS 31062–050 is known to be a so-called CEMP-r/s star, which exhibits large excesses of s-process elements such as barium (Ba) and lead (Pb), as well as a significant enhancement of europium (Eu) that cannot be explained by conventional s-process production in Asymptotic Giant Branch star models. Our analysis of the high-resolution spectrum for this object has determined, for the first time, the abundances of Ir and Os, elements in the third peak of the r-process nucleosynthesis. They also exhibit significant excesses relative to the predictions of standard s-process calculations. These two elements are not detected in a similar-quality spectrum of LP 625–44; the derived upper limits on their abundances are lower than the abundances in CS 31062–050. We compare the observed abundance patterns of neutron-capture elements, including Os and Ir, in these two stars with recent model calculations of the s-process, and discuss possible interpretations.

Subject headings: nuclear reactions, nucleosynthesis, abundances — stars: abundances — stars: Population II, — stars: AGB and post-AGB — stars: individual (CS 31062–050) — stars: individual (LP 625–44)

²National Astronomical Observatory, Mitaka, Tokyo, 181-8588, Japan; email: aoki.wako@nao.ac.jp

³Dipartimento di Fisica Generale dell'Università di Torino, via P. Giuria 1, 10125 Torino, Italy; bisterzo@ph.unito.it, gallino@ph.unito.it

⁴Forschungszentrum Karlsruhe, Institute fuer Kernphysik, P.O. Box 3640, D-76021 Karlsruhe, Germany

⁵Centre for Stellar and Planetary Sciences, School of Mathematical Sciences, Monash University, Building 28, Victoria 3800, Australia

⁶Dept. of Physics & Astronomy, CSCE: Center for the Study of Cosmic Evolution, and JINA: Joint Institute for Nuclear Astrophysics, Michigan State University, E. Lansing, MI 48824; beers@pa.msu.edu

⁷Research School of Astronomy and Astrophysics, The Australian National University, Mount Stromlo Observatory, Cotter Road, Weston, ACT 2611, Australia; email: jen@mso.anu.edu.au

⁸Department of Physics and Astronomy, The Open University, Walton Hall, Milton Keynes, MK7 6AA, UK; email: stsangarides@gmail.com

⁹Present address: Centre for Astrophysics Research, STRI and School of Physics, Astronomy and Mathematics, University of Hertfordshire, College Lane, Hatfield AL10 9AB, United Kingdom; s.g.ryan@herts.ac.uk

1. Introduction

Recent abundance analyses of Carbon-Enhanced Metal-Poor (CEMP) stars have provided a unique opportunity to investigate the abundance patterns produced by s-process nucleosynthesis at low metallicity (e.g., Norris et al. 1997; Hill et al. 2000). Of particular importance, in the past several years abundance measurements of neutron-capture elements have been extended to cover a wide range of atomic numbers, including heavy species such as lead (Pb; e.g. Aoki et al. 2000; van Eck et al. 2001) and bismuth (Bi; e.g. Ivans et al. 2005). One interesting class of objects that have recently been identified are the so-called r/s stars (e.g. Hill et al. 2000; Cohen et al. 2003; Beers & Christlieb 2005; Jonsell et al. 2006). These stars exhibit large enhancements of the neutron-capture elements, whose overall abundance patterns can be explained by the s-process, but whose abundance of the r-process element Eu is much higher than the value predicted by conventional s-process nucleosynthesis models². All of the presently recognized r/s stars also exhibit large carbon enrichment ($[C/Fe] \gtrsim +1.0$); Beers & Christlieb (2005) refer to these as CEMP-r/s stars.

The observed excesses of s-process elements in CEMP stars are usually explained by the yields of Asymptotic Giant Branch (AGB) stars (see Herwig 2005 for a recent review). Since most CEMP stars observed today are not in their AGB phase, it is usually assumed that the AGB star responsible for the s-process (and carbon enhancement) was once the primary of a binary system, and the elements formed by it were transferred by a stellar wind to a lower-mass companion (the star now observed) prior to the primary evolving to become a faint white dwarf. One possible scenario to explain CEMP-r/s stars is to assume that the parent cloud of the binary system was already enriched in the r-process elements. The r-process nucleosynthesis source(s), presumably core-collapse supernovae, would leave an elemental imprint of its products on such very low-metallicity objects, according to the above interpretation. One important observational constraint is that a significant fraction of very metal-poor s-process-enhanced stars are in fact r/s stars. For instance, Jonsell et al. (2006) list 17 r/s stars among 24 s-process-enhanced objects. This stands in contrast to the fact that r-process-enhanced ($[Eu/Fe] \gtrsim +1.0$) stars with no excess of s-process elements are quite rare among very metal-poor stars ($\sim 5\%$; Barklem et al. 2005). The large fraction of r/s stars among s-process-enhanced stars is not explained by assuming that these stars accidentally had large overabundances of r-process elements, but suggests that a close relationship may exist between the s- and r-processes that form the abundance patterns of r/s stars.

The interest in r/s stars has been rapidly growing in recent years. However, the classification of

¹Based on data collected at the Subaru Telescope, which is operated by the National Astronomical Observatory of Japan.

²The solar-system isotopic abundances of neutron-capture elements are decomposed using s-process models. The fraction of r-process contribution is estimated by subtracting the s-process contribution from the total abundances. The terms s-process elements and r-process elements mean the elements whose solar-system abundances are mostly explained by corresponding processes. For instance, more than 94% of Eu in the Solar System is yielded by the r-process, according to Arlandini et al. (1999) and Simmerer et al. (2004).

such objects mostly relies on the relatively easily measured Eu abundance, although the abundances of elements between Gd and Lu also provide constraints on the origin of neutron-capture elements for a small number of stars (e.g., CS 29497-030; Ivans et al. 2005). In order to better estimate the relative contributions of the s- and r-processes in r/s stars, it is important to increase the number of such stars with available abundance measurements for elements in the third peak of the r-process nucleosynthesis (Os and Ir, whose r-process fractions in solar-system material are 91.6 and 98.8%, respectively, according to Simmerer et al. (2004)).

We have investigated high-resolution ultraviolet-blue spectra of two CEMP subgiants, CS 31062–050 and LP 625–44, whose abundance patterns were studied relatively well by previous work (Norris et al. 1997; Aoki et al. 2000, 2002a,b; Johnson & Bolte 2004). These stars have quite similar atmospheric parameters and carbon enhancements. Moreover, variations of radial velocities have been detected in both of these stars, indicating that they both belong to binary systems. In this Letter, the abundances of Os and Ir in CS 31062–050, as well as upper limits on these elements in LP 625–44, are reported. The abundance patterns of these stars are then compared to the predictions of modern s-process nucleosynthesis models.

2. Observations and Analyses

High-resolution spectra (3100–4700 Å) of CS 31062–050 and LP 625–44 were obtained in August 2002 with the High Dispersion Spectrograph (HDS: Noguchi et al. 2002) of the Subaru Telescope. The spectra were used to measure the Eu isotope ratios in these stars in our previous work (Aoki et al. 2003): see §2 of that paper for details of the observations and data reduction. The photon counts (per 0.9 km s⁻¹ pixel) at 3515 Å and 4260 Å, where measurable Ir and Os lines exist, are 8300 and 25000 for CS 31062–050 and 6800 and 20500 for LP 625–44, respectively. Figure 1 shows the spectra of these stars in the region of these spectral lines. The high resolving power ($R = 90,000$) achieved in these observations is very important to resolve the Ir line from the other absorption features. In this paper, we also use the red spectrum of CS 31062–050 obtained by Aoki et al. (2006) to determine the Ba abundance.

We carry out LTE abundance analyses for CS 31062–050 and LP 625–44, using the model atmospheres of Kurucz (1993), and adopting the atmospheric parameters determined by Johnson & Bolte (2004) and Aoki et al. (2002a), respectively (Table 1). One reason for adopting these values from previous work is to combine our abundances of Os and Ir with previous results for other elements. Note that the effective temperatures estimated from the $V - K$ colors of these two stars, adopting the scale of Alonso, Arribas, & Martínez-Roger (1999), are 150–180 K higher than the values adopted here (5500 K). However, this small difference does not significantly affect the relative abundance patterns discussed in this Letter.

We applied the spectrum synthesis technique to the Ir $\lambda 3513$ Å and Os $\lambda 4260$ Å lines, as illustrated in Figure 1. The oscillator strengths of these lines are taken from the list of Hill et al.

(2002). We note that their oscillator strength of the Os line is confirmed by the recent measurements of Quinet et al. (2006). As a test, we also carry out analyses of Ir and Os, based on these same lines, for the spectra of CS 31082–001 (Hill et al. 2002) and HD 6268 (Honda et al. 2004), and find good agreement between our results and those of these authors (the differences are smaller than 0.1 dex). The Ir and Os lines are clearly detected in the spectrum of CS 31062–050, and abundances of these species are determined for this star, while only upper limits on the abundances of these species are estimated for LP 625–44. The results are listed in Table 1.

We also measure abundances for six heavy neutron-capture elements, Ba, La, Eu, Hf, and Pb, for both stars. The Ba abundance of CS 31062–050 is re-determined using the $\lambda 5853 \text{ \AA}$ and $\lambda 6141 \text{ \AA}$ lines, which are much weaker, and less sensitive to the effect of hyperfine splitting than the resonance lines, and thus preferable for abundance measurements. The Ba abundance we derive is 0.2 dex lower than that reported by Johnson & Bolte (2004), who obtained an extremely large enhancement of this element compared to other neutron-capture species. Our measurement, using different spectral lines, confirms the large excess of Ba, although the enhancement is not as large as reported by Johnson & Bolte (2004). We confirm a good agreement between our results and those of Johnson & Bolte (2004) for other elements in CS 31062–050. We note that the Yb abundance is determined using the $\lambda 3476 \text{ \AA}$ line, rather than the very strong $\lambda 3692 \text{ \AA}$ line, in order to avoid uncertainties due to damping effects and isotope splitting. The same line is used to determine the Yb abundance of LP 625–44. Aoki et al. (2002a) analyzed the $\lambda 3692 \text{ \AA}$ line in this star, but only obtained a very uncertain result. The La abundance of LP 625–44 is re-determined using the line data provided by Lawler et al. (2001). The errors given in Table 1 are the uncertainties due to fitting of synthetic spectra. Errors due to the uncertainties of atmospheric parameters are of the order of 0.1–0.15 dex, as estimated by previous work for heavy neutron-capture elements (e.g., Aoki et al. 2002a). It should be noted that no stronger constraint on the upper limit of Th abundance in CS 31062–050 than that of Johnson & Bolte (2004) is obtained, because of the severe blending of CH molecular features with the Th II $\lambda 4019 \text{ \AA}$ line, although the spectral resolution of our data is higher than theirs.

In the following discussion we adopt the results of the present analysis for Ba, Os, and Ir for CS 31062–050, and those of Johnson & Bolte (2004) for other elements. For LP 625–44, the abundance of La and Yb, as well as the upper limits on the Os and Ir abundances, determined by the present work, are combined with the results of Aoki et al. (2002a).

3. Comparison with Modern s-Process Models

Figure 2 shows a comparison of the observed abundance patterns of heavy neutron-capture elements for CS 31062–050 and LP 625–44 with the FRANEC model calculations (Straniero et al. 2003; see also Zinner et al. 2006), which are obtained for an AGB star of mass $1.3 M_{\odot}$ with metallicity of $[\text{Fe}/\text{H}] = -2.4$ and $[\text{Fe}/\text{H}] = -2.7$, respectively. The dotted lines indicate the results of the calculation for which the abundance pattern of neutron-capture elements in solar-system

material, scaled to the model metallicity, is assumed for the initial composition (here we refer to this as the standard model). In the comparisons of the model calculations with observational data, we give a priority to the abundances of the elements near the three peaks of the s-process (Zr, La–Nd, and Pb; we did not give a priority to Ba because of the difficulty mentioned above). The abundance pattern of CS 31062–050 for La–Sm and Pb agrees well with the model prediction, while Eu, Gd, and Er–Hf exhibit excesses. The Os and Ir abundances obtained by the present work are also clearly higher than the predictions of the standard model.

The observed excesses of Os and Ir in CS 31062–050, as well as other elements such as Eu, can be explained by assuming a large contribution to the atmosphere of this star due to r-process nucleosynthesis. The abundance pattern of heavy neutron-capture elements produced by the (main) r-process is known to agree very well with that of the r-process component in solar-system material (e.g. Sneden et al. 2003). Hence, we assume excesses of the neutron-capture elements with the solar-system r-process abundance pattern as the initial abundances for the calculation. A good fit to the observed abundances of Eu, Os, and Ir is found when the r-process abundance pattern, normalized to $[\text{Eu}/\text{Fe}] = +1.5$, is assumed for the initial composition of this star. The abundance pattern obtained by this calculation is shown by the solid line in Figure 2. This assumption for the initial composition does not significantly affect the final abundances of light neutron-capture elements (Sr, Y, and Zr), nor the heavy s-process elements (Ba–Sm) and Pb, because the contribution of the s-process is dominant. In contrast, the abundances of Eu, Ir, Os, and several other heavy neutron-capture elements (Gd–Yb), are significantly enhanced by this assumption for the initial composition. We note that the Pd abundance in CS 31062–050 is better explained by the corresponding AGB model with no initial r-process enrichment. However, the Pd abundance produced by the r-process could be lower than the “r-process component” of the solar-system Pd abundance. According to the abundance patterns found in r-process-enhanced metal-poor stars (e.g. Hill et al. 2002; Sneden et al. 2003), the yields of the main r-process has $[\text{Pd}/\text{Eu}] \sim -0.5$, while the r-process component in solar-system material has $[\text{Pd}/\text{Eu}] = -0.25$. This suggests that the initial Pd abundance assumed in our calculation is overestimated by about 0.2 dex.

The overall abundance pattern of CS 31062–050, including Eu, Os and Ir, is fit better by our model assuming excesses of r-process elements in the initial abundances. The abundance pattern, in particular for Os and Ir, cannot currently be explained without a large contribution of the r-process to the neutron-capture elements in this star. Some elements still show significant deviation from this model (e.g. Er–Hf), indicating that our model assuming the excesses of neutron-capture elements with the solar-system r-process abundance pattern is not a final solution. However, the abundances of Os and Ir, which are almost pure r-process elements, clearly request a large contribution of the r-process or of some unknown process to CS 31062–050 (see next section). For LP 625–44, we could only obtain upper limits on the Os and Ir abundances; they are both lower than the measured abundances of these species for CS 31062–050. From this result, we can only conclude that the contribution of the r-process to the Os and Ir in LP 625–44, if any, is smaller than that in CS 31062–050. The higher $[\text{La}/\text{Eu}]$ of this star ($[\text{La}/\text{Eu}] = +0.74$), as compared to that of CS 31062–050

($[\text{La}/\text{Eu}] = +0.33$), also supports this conclusion. It should be noted that the model predictions are scaled to fit the three s-process-element abundance peaks, and the agreement is not good for La–Hf. However, the relatively low abundance ratio of Pb with respect to the second s-process peak (e.g., Ba, La) in LP 625–44, as well as in several other objects, is a problem also found by other recent observations (e.g. Aoki et al. 2002b), and further s-process modeling for such objects is desired.

4. Discussion and Concluding Remarks

There is no astrophysical model that can well explain the abundance pattern of CEMP r/s stars. The model is required to explain the following two observational facts: (1) More than ten CEMP-r/s stars that exhibit very large excesses of Eu ($[\text{Eu}/\text{Fe}] > +1$) are already known, while only a few r-process-enhanced stars without excesses of s-process elements are known; (2) The CEMP-r/s stars exhibit larger enhancements of heavy neutron-capture elements, on average, than the stars having only s-process enhancements (Jonsell et al. 2006). To account for these constraints, a modified s-process model which yields abundance patterns that are quite different from those of standard models might be preferred, as has been discussed by previous authors (see Jonsell et al. 2006, and references therein). However, the high Os and Ir abundances, as well as the high Eu abundance, found in CS 31062–050 appear to exclude this possibility, because no s-process model known to date predicts such high yields of these elements. We confirmed that Os and Ir are not efficiently produced by our AGB models, even if model parameters (initial mass, efficiency of mixing to produce the neutron source ^{13}C) are significantly changed. If a single astrophysical process capable of producing the observed abundance patterns of r/s stars exists, it must be significantly different than s-process production by AGB stars known so far.

As mentioned in the previous section, the abundance pattern of neutron-capture elements in CS 31062–050 is better accounted for by a model that assumes an initial composition for the binary system with large excesses of heavy elements having a scaled solar r-process abundance pattern. Thus, we argue that this system was formed from a parent cloud polluted by a supernova that yielded r-process elements, which might have also triggered the formation of next-generation low-mass binary stars (Vanhala & Cameron 1998), while the s-process elements were provided by the former primary star during its AGB phase. A possible alternative scenario is to assume that pollution of CS 31062–050 with r-process-enhanced material took place after s-process nucleosynthesis. This might be the case if the progenitor was an 8–10 M_{\odot} star that underwent s-process nucleosynthesis during its AGB phase, followed by the production of r-process elements during its subsequent supernova explosion (Wanajo et al. 2006). However, it is not yet clear how much of the s-process material may be mixed within the envelope of these stars (Doherty 2006; Siess 2006). These two scenarios are, unfortunately, not easily distinguished by the elemental abundance pattern of the low-mass stars that are currently observed, because the majority of the r-process nuclei for which excesses are assumed for the initial composition are not subject to the s-process. Hence, the r- and

s-processes behave as almost independent contributors to the final yields.

Finally, we point out that, although CS 31062–050 and LP 625–44 have similarly large excesses of carbon and neutron-capture elements, their elemental abundance patterns exhibit non-negligible differences. CS 31062–050 exhibits a large excess of Pb, as expected from s-process models (Aoki et al. 2002b; Johnson & Bolte 2004), while LP 625–44 has a smaller enhancement of Pb (Aoki et al. 2000, 2002a). The [La/Eu] ratios show some difference, as mentioned in §3. In addition, the sodium (Na) abundance is significantly different between the two stars (Aoki et al. 2002a, 2006). These differences suggest that the process(es) responsible for the production of these elements may not be the same in these two stars. More detailed comparisons of the elemental abundances for these two stars are strongly desired.

W.A. is grateful for useful discussions with Drs. N. Iwamoto, T. Kajino, and G. J. Mathews. R.G. acknowledges support by the Italian MIUR-FIRB Project "Astrophysical Origin of Heavy Elements beyond Fe" T.C.B. acknowledges partial support from a series of grants awarded by the US National Science Foundation, most recently, AST 04-06784, as well as from grant PHY 02-16783; Physics Frontier Center/Joint Institute for Nuclear Astrophysics (JINA). J.E.N. acknowledges support from Australian Research Council grant DP0342613.

REFERENCES

- Alonso, A., Arribas, S., & Martínez-Roger, C. 1999, *A&AS*, 140, 261
- Aoki, W. et al. 2002a, *PASJ*, 54, 427
- Aoki, W., Beers, T. C., Christlieb, N., Norris, J. E., Ryan, S. G., Tsangarides, S. 2006, *ApJ*, submitted
- Aoki, W., Norris, J. E., Ryan, S. G., Beers, T. C., & Ando, H. 2000, *ApJ*, 536, L97
- Aoki, W., Ryan, S. G., Norris, J. E., Beers, T. C., Ando, H., & Tsangarides, S. 2002b, *ApJ*, 580, 1149
- Aoki, W., Ryan, S. G., Iwamoto, N., Beers, T. C., Norris, J. E., Ando, H., Kajino, T., Mathews, G.J., & Fujimoto, M. Y. 2003, *ApJ*, 592, L67
- Arlandini, C., Käppeler, F., Wisshak, K., Gallino, R., Lugaro, M., Busso, M. & Straniero, O. 1999, *ApJ*, 525, 886
- Barklem, P. S., et al. 2005, *A&A*, 439, 129
- Beers, T. C., & Christlieb, N. 2005, *ARA&A*, 43, 531
- Cohen, J. G., Christlieb, N., Qian, Y. -Z., & Wasserburg, G. J. 2003, *ApJ*, 588, 1082

- Doherty C. 2006, in Proc. IX Torino Workshop in Granada (eds. I. Dominguez and C. Abia), Mem. Soc. Atron. It., in press
- Herwig, F. 2005, ARA&A, 43, 435
- Hill, V., et al. 2000, A&A, 353, 557
- Hill, V., et al. 2002, A&A, 387, 560
- Honda, S., Aoki, W., Kajino, T., Ando, H., Beers, T. C., Izumiura, H., Sadakane, K., & Takada-Hidai, M. 2004, ApJ, 607, 474
- Ivans, I. I., Sneden, C., Gallino, R., Cowan, J. J., & Preston, G. W. 2005, ApJ, 627, L145
- Johnson, J. A., & Bolte, M. 2004, ApJ, 605, 462
- Jonsell, K., Barklem, P. S., Gustafsson, B., Christlieb, N., Hill, V., Beers, T. C., & Holmberg, J. 2006, A&A, 451, 651
- Kurucz, R. L., 1993, CD-ROM 13, ATLAS9 Stellar Atmospheres Programs and 2 km/s Grid (Cambridge: Smithsonian Astrophys. Obs.)
- Lawler, J. E., Bonvallet, G., & Sneden, C. 2001, ApJ, 556, 452
- Lodders, K. 2003, ApJ, 591, 1220
- Noguchi, K., Aoki, W., Kawanomoto, S., et al. 2002, PASJ, 54, 855
- Norris, J. E., Ryan, S. G., & Beers, T. C. 1997, ApJ, 488, 350
- Quinet, P., Palmeri, P., Biéumont, É., Jorissen, A., van Eck, S., Svanberg, S., Xu, H. L., & Plez, B. 2006, A&A, 448, 1207
- Siess, L. 2006, A&A, 448, 717
- Simmerer, J., Sneden, C., Cowan, J. J., Collier, J., Woolf, V. M., & Lawler, J. E. 2004, ApJ, 617, 1091
- Sneden, C., Preston, G. W., & Cowan, J. J. 2003, ApJ, 592, 504
- Straniero, O. Dominguez, Cristallo, S., Gallino, R. Publ. Astron. Soc. Australia 2003, 20, 389
- Van Eck, S., Goriely, S., Jorissen, A. & Plez, B., 2001, Nature, 412, 793
- Vanhala, H. A. T., & Cameron, A. G. W. 1998, ApJ, 508, 291
- Wanajo, S., Nomoto, K., Iwamoto, N., Ishimaru, Y., & Beers, T. C. 2006, ApJ, 636, 842
- Zinner, E., Nittler, L., Gallino, R., Karakas, A., Lugaro, M., Straniero, O., Lattanzio, J.C., 2006, ApJ, in press.

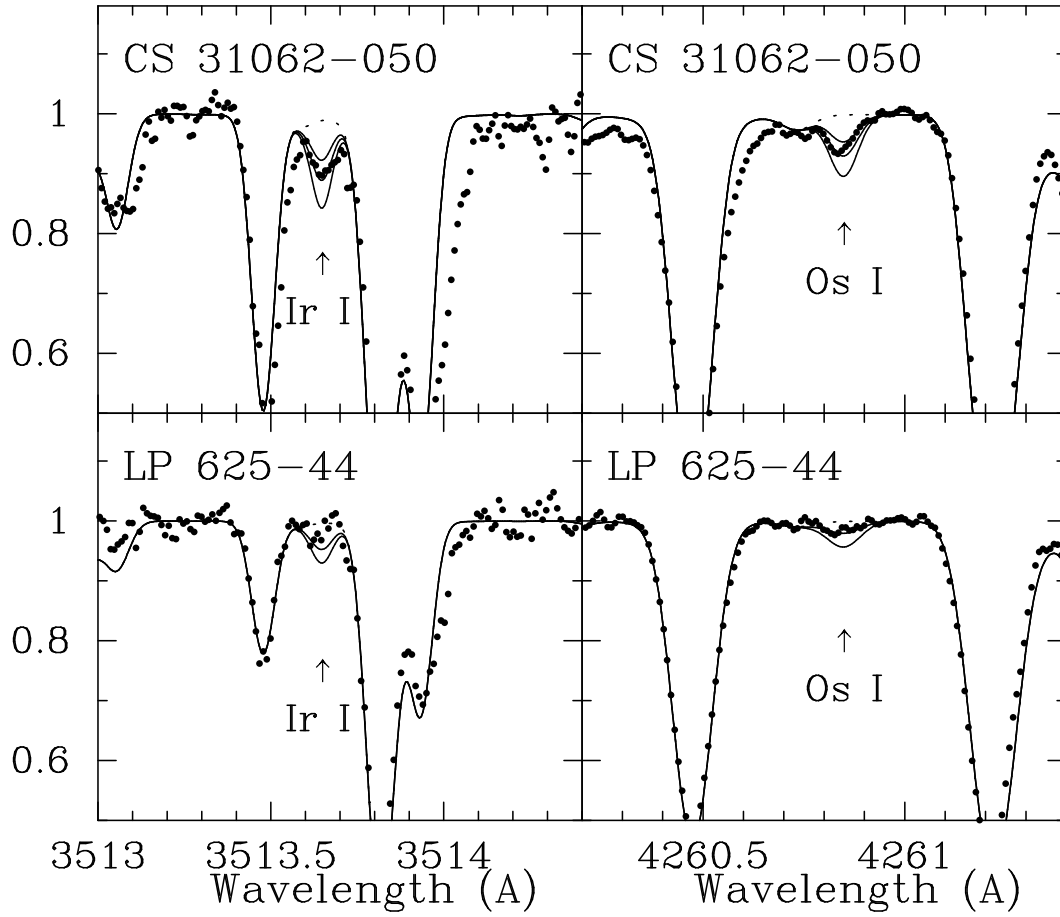


Fig. 1.— Comparisons of synthetic spectra for the Ir I $\lambda 3513 \text{ \AA}$ and the Os I $\lambda 4260 \text{ \AA}$ features with the observed ones in CS 31062–050 and LP 625–44. The assumed abundances are $\log \epsilon(\text{Os}) = 0.75 \pm 0.20$ and $\log \epsilon(\text{Ir}) = 0.35 \pm 0.20$ for CS 31062–050, while those for LP 625–44 are $\log \epsilon(\text{Os}) = 0.60$ (adopted upper limit) and 0.25 (for a comparison), and $\log \epsilon(\text{Ir}) = 0.15$ (adopted upper limit) and -0.05 (for a comparison). The dotted lines indicate the spectra calculated assuming no Os or Ir.

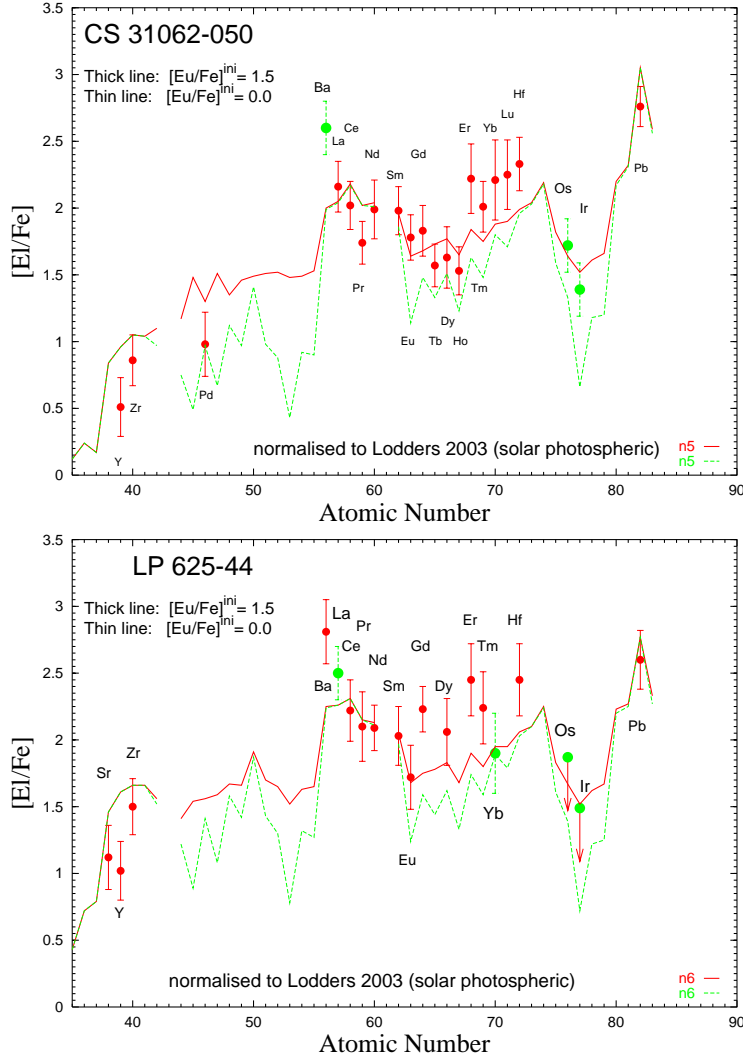


Fig. 2.— Comparison of the calculated abundance patterns with the observational results. The abundances are normalized to the solar photospheric abundances provided by Lodders (2003). In the upper panel, the Ba, Os, and Ir abundances of CS 31062–050 measured in the present work and those of other elements adopted from Johnson & Bolte (2004) are shown along with the AGB s-process models for an initial mass of $1.3 M_{\odot}$, $[Fe/H] = -2.42$, and the ST/10 case (a choice of ^{13}C concentration in the ^{13}C pocket). The solid line indicates the model assuming the initial enhancement of r-process elements normalized to $[Eu/Fe] = +1.5$, while the dashed line is the model predictions without such initial enhancements (see text for details). The lower panel shows the same comparison, but for LP 625–44. The La and Yb abundances, and the upper limits of Os and Ir abundances, determined by the present work are shown along with the abundances of other elements adopted from Aoki et al. (2002a). The models assuming an initial mass of $1.3 M_{\odot}$, $[Fe/H] = -2.70$, and ST/30 are shown in this diagram.

Table 1. ATMOSPHERIC PARAMETERS AND ABUNDANCES RESULTS

	CS 31062–050				LP 625–44			
T_{eff} (K)	5500				5500			
$\log g$ /[cm s ⁻²]	2.7				2.5			
[Fe/H]	–2.3				–2.7			
v_{turb} (km s ⁻¹)	1.3				1.2			
	$\log \epsilon$	[X/Fe]	σ	$\log \epsilon_{\text{JB04}}^{\text{a}}$	$\log \epsilon$	[X/Fe]	σ	$\log \epsilon_{\text{A02}}^{\text{a}}$
Ba	2.35	+2.60	0.2	2.61	2.31	+2.86	0.2	2.31
La	0.95	+2.24	0.06	0.93	0.91	+2.50	0.07	0.90
Eu	0.01	+1.91	0.05	–0.07	–0.44	+1.76	0.05	–0.48
Yb	0.5:	+1.8:	0.3	0.76	0.3:	+1.9:	0.3	...
Hf	0.67	+2.21	0.1	0.67	0.55	+2.39	0.1	0.48
Os	0.75	+1.72	0.2	...	< 0.60	< 1.87
Ir	0.35	+1.39	0.2	...	< 0.15	< 1.49
Pb	2.45	+2.87	0.1	2.46	1.95	+2.67	0.1	1.90

^aResults obtained by Johnson & Bolte (2004) and Aoki et al. (2002a).